Structural Deterioration Localisation Using Enhanced Autoregressive Time-Series Analysis

Benyamin Monavari[1], Tommy H.T. Chan[2], Andy Nguyen[3], David P. Thambiratnam[2], Khac Duy Nguyen[4]
[1] *Ph.D., Queensland University of Technology, Queensland, Australia, Email:* b.monavari@qut.edu.au
[2] Professor, Queensland University of Technology, Queensland, Australia
[3] Lecturer, University of Southern Queensland, Queensland, Australia
[4] Research Fellow, Queensland University of Technology, Queensland, Australia

Abstract

Irrespective to how well structures were built, they all deteriorate. Herein, deterioration is defined as a slow and continuous reduction of structural performance, which if prolonged can lead to damage. Deterioration occurs due to different factors such as ageing, environmental and operational (E&O) variations including those due to service loads. Structural performance can be defined as load-carrying capacity, deformation capacity, service life and so on. This paper aims to develop an effective method to detect and locate deterioration in the presence of E&O variations and high measurement noise content. For this reason, a novel vibration-based deterioration assessment method is developed. Since deterioration alters the unique vibration characteristics of a structure, it can be identified by tracking the changes in the vibration characteristics. This study uses enhanced autoregressive (AR) time-series models to fit the vibration response data of a structure. Then, the statistical hypotheses of chi-square variance test and two-sample t-test are applied to the model residuals. To precisely evaluate changes in the vibration characteristics, an integrated deterioration identification (*DI*) is defined using the calculated statistical hypotheses and a Hampel filter is used to detect and remove false positive and negative results. Model residual is the difference between the predicted signal from the time series model and the actual measured response data at each time interval. The response data of two numerically simulated case studies of 3-storey and 20-storey reinforced concrete (RC) shear frames contaminated with different noise contents demonstrate the efficacy of the proposed method. Multiple deterioration and damage locations, as well as preventive maintenance actions, are also considered in these case studies. Furthermore, the method was successfully verified utilizing measured data from an experiment carried out on a box-girder bridge (BGB) structure.

Keywords: Deterioration identification; AR residual; SHM; Vibration-based, Statistical hypothesis.

1. Introduction

Due to the rapid increase in the number of ageing civil structures in recent years, many structural health monitoring (SHM) systems are now being developed around the world to look after these infrastructure stocks. The accumulation of deterioration in conjunction with poor preventive maintenance plans has led many structures to a lower level of structural performance, potential damage and even on the verge of collapse or partial failure. Herein, the slow and continuous process of reduction in structural performance due to ageing, varying service loads and environmental factors is defined as deterioration[1]. The causes of deterioration process have been comprehensively investigated by Val and Stewart[2] and Liu[3]. To prevent the accumulation of deterioration and leading to damage, preventive maintenance actions are required, which in turn require detecting and locating the structural deterioration. Preventive maintenance actions improve the performance of deteriorated structures and extend their life expectancy[4].

Detecting and locating deterioration in structures are crucial. However, due to slight changes in dynamic characteristics of deteriorated structures, unknown input excitations, significant level of measurement noise, and change in operational conditions, it is still quite a challenge to identify deterioration, and only few researchers have studied structural deterioration assessment. Sanchez et al.[5] defined and examined four cases representing health cases related to deterioration of the reinforcement and concrete cover. Many other different corrosion models have been investigated to predict the effect of the corrosion of steel in concrete and to estimate the corrosion rate (for example see (Berto et al.[6]; Gulikers[7]; Morinaga[8])). Wang and Liu[9] modelled the cracking and spalling of the concrete cover due to corrosion of reinforcing bars by defining the effective depth of concrete cover to consider the loss of confinement of concrete cover. Some researchers defined deterioration as a continuous loss of cross-sectional area in time (Okasha & Frangopol[10]). For example, Barone et al.[11] considered annual deterioration rate (ADR) for cross-sectional area to be equal to 2×10^{-3} in a single component subjected to an increasing axial force. Zhou[12] defined deterioration as a reduction of a small portion of concrete from the top surface of a specimen when the deterioration is the result of spalling of the concrete. These assumptions might be suitable for assessing one component with the same imposing load; however, it is not accurate for a building with many components and different loadings. As a result, a novel and accurate procedure for deterioration assessment of the current health state of buildings is necessary.

Since the dynamic characteristics (natural frequencies, mode shapes, and damping properties) of a structure are correlated with their material and geometric properties, accumulated deterioration and damage alter their vibration characteristics. Hence, capturing changes in the vibration characteristics would similarly allow deterioration detection[5]. It is, however, worth noting that the changes due to deterioration are much subtler than those due to damage. Therefore, it is very challenging to detect deterioration, particularly using output-only based methods even though these methods are often preferred in practice due to their applicability to in-service structures.

Reviews of SHM methods, as captured by Doebling et al.[13], Carden and Fanning[14] and Chan and Thambiratnam[15], show that most SHM studies have used vibration-based methods for damage detection, but not for detecting deterioration. Vibration-based damage detection

(VBDD) methods have been extensively investigated in the past three decades[13-19]. The literature also indicates that time-series based methods are among the most promising output-only VBDD methods in structural health monitoring. For instance, Mosavi et al.[20] concluded that time-series based methods are sensitive and reliable techniques for structural assessment. Kadakal & Yuzugullu[21] and Pardoen[22] claimed that these techniques perform well under ambient vibration conditions. Recently, the authors of this present paper successfully developed time-series based deterioration assessment[23-25]. These methods have been proved to be successful in detecting deterioration but did not give any information on its location.

Time-series methods compare baseline and assessment phases of a structure to identify changes in the structure. Many time series methods have been proposed for damage detection, including AR[26-30], ARMA (Carden and Brownjohn[31], Pandit et al.[32] and Garcia and Roberto[33]) and ARMAX (Mei et al.[34], Ngoan and Gül[35] and Ay and Wang[36]) models. Among these methods, AR model has been found to be practical and reliable due to its capability of detecting damage in ambient vibration condition. For instance, Fugate et al.[26] used AR model residuals as a damage feature, while Sohn et al.[28], De Lautor and Omenzetter[29,30] and Zugasti et al.[37] presented VBDD methods based on AR model coefficients. Omenzetter and Brownjohn[38] used coefficients of time-series models to detect structural changes or damage. Zhang[39] could detect and localize damage in structures using AR time-series residuals under ambient vibration. Wang et al.[40] used enhanced AR coefficients to detect structural damage in the presence of noise. Zhang and Mita[41] used the distance measure of AR models to detect and locate damage. They also used a pre-whitening filter to improve the accuracy of their damage detection method. Although these methods have been extensively used in VBDD[29-39], none of them has been used in deterioration detection.

This paper aims to develop a novel vibration-based deterioration assessment method. It first presents an innovative data normalization procedure. Then, an improved time-series model with a novel optimal model order (OMO) estimation technique is developed to estimate time-series model orders. Next, *DI* is defined using the integrated statistical hypotheses of the chi-square variance test and two-sample t-test on model residuals. A Fisher-criterion-based algorithm is then developed to estimate the deterioration location. Applicability of the proposed method is demonstrated through numerical simulations of 20-storey and 3-storey concrete frame structures and sensor data from an experiment carried out on a BGB structure. Details of these parts are presented in the next two sections of this paper before discussion and conclusion are made in the last two sections.

2. Methodology

2.1. Data normalization

For time series analysis, the structural response data are assumed to be stationary. Nevertheless, recorded data under ambient excitations are often non-stationary. In order to use these data in time series based methods, normalization procedure is a necessary preprocessing step which accounts for the effects of the various E&O conditions on the structural dynamics[17]. Details of the used normalization procedure can be found in the recent publication of the present authors[17]. Its summary is as follows.

Data collected from the SHM systems are standardized:

$$\hat{x}_i = \frac{x_i - \bar{x}}{\sigma} \tag{1}$$

where x_i indicates the amplitude of measured acceleration response data; $\bar{x}$, σ and $\hat{x}_i$ are the mean, standard deviation (STD) and the standardized signal of x_i, respectively.

A noise-contaminated high-frequency content data increase the effect of E&O variations as well as the model residuals[25]. Hence, the data are filtered with low-pass Chebyshev filter which removes the high-frequency content. More information can be obtained from Smith[42]. In order to minimize the cross-correlation among multiple excitations, a pre-whitening filter is also applied to pre-whiten (de-correlate) the sensor signals from the vibration structure. As the excitations acting on real structures, such as wind, traffic loads and earthquakes, are correlated, the utilized de-correlation technique plays a key role in the accuracy of the proposed deterioration assessment method since it eliminates redundancy and reduces noise[43].

2.2. AR time-series model

In the proposed method, deterioration identification can be achieved from changes in time-domain response data. The AR statistical model is used to predict the signal in the current state of a structure using the past response of the structure. An AR model can be given as follows:

$$x_k = \sum_{i=1}^{p} \Phi_i^x x_{k-i} + e_k^x \tag{2}$$

where p is the model order (which will be explained in the next section); x_{k-i} represents the $(k-i)^{th}$ previous response; Φ_i^x is the i^{th} AR coefficient of the corresponding previous response, and e_k^x is the residual error of the model. Figure 1 shows a dataset and corresponding well fitted AR model.

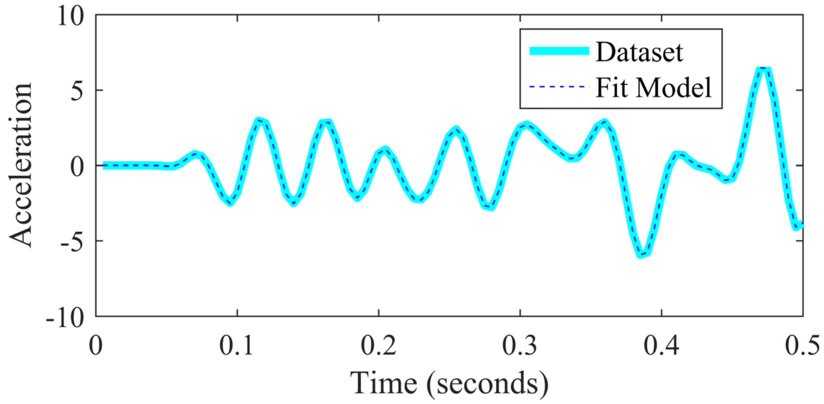

Figure 1. AR model fitted to a dataset using one-step-ahead error prediction

2.2.1. Model identification

Each time-series model requires a model order which is an unknown value. A model requires to be low enough (simplicity) to be generalized to a wide range of datasets and to be high enough (minimum residual) to capture the dynamic characteristics of a structure. In other words, a too simple fit increases the residual and a higher model order may not be generalized to the other datasets. The model orders specify the number of allocated unknown parameters to the models so as to predict the response of structures. Time-series model orders play a crucial role in detecting structural changes. Figueiredo et al.[44] evaluated the effect of different model orders on the assessment of structural changes. To estimate the model orders, some methods use information criterion techniques such as Akaike and Bayesian information criteria, while others check the autocorrelation and cross-correlation of model residuals[45]. For instance, Entezami and Shariarmadar[46] proposed an iterative model order estimation method based on the correlation of model residuals using Ljung-Box Q-test. Nevertheless, these techniques are mostly suitable for detecting damage but not deterioration. As the changes in the response of structures due to deterioration are much smaller than those caused by damage, the current techniques for estimating model orders which are widely used in damage detection, cannot be directly used.

Recently, a novel technique for deterioration assessment methods, which is named best model order (BMO), was proposed in one of the publications of the present authors[25]. In the present paper, the BMO technique is further developed (i.e. OMO technique) which yields more sensitive deterioration features. In the OMO technique, a new λ criterion is proposed to derive more accurate model order for deterioration assessment purposes. For a reasonable estimation, datasets in the baseline state should be selected from different E&O conditions such as different temperatures. Undoubtedly, the more datasets in the baseline, the more accurate the result. The OMO technique is described in the following steps.

1) Normalizing all the selected datasets

2) Selecting the first dataset and estimating AR models with different model orders

3) Obtaining STD ratio of model residuals between the estimated models and the other normalized datasets.

$$R_{(i,j)} = \frac{\sigma(e_{(i,j)})}{\sigma(e_{(1,j)})} \tag{3}$$

where $i = 1, 2, ..., n$; n is the number of datasets in baseline state; $j = 1, 2, ..., m$; and m is a high enough limitation for model order.

4) Calculating residuals' root mean square (RMS_e) and mean (γ parameter)

$$RMS_{e_{(i,j)}} = \sqrt{\frac{1}{k}\sum_{l=1}^{k}(e_{(i,j)}^{l})^2} \tag{4}$$

where $e_{(i,j)}^{k}$ is residual error at the k^{th} signal value.

$$\gamma = \mu(\mathbf{RMS}) \tag{5}$$

5) Estimating the minimum model order which minimizes γ parameter. This model order, which ensures the minimal of residuals, is the minimum required model order to capture structural dynamic characteristics.

6) Determining λ parameter and finding the model order which minimizes λ value and is higher than previously estimated minimum model order. The minimum λ value corresponds to model order having similar *R* values in average for all the used datasets. Hence, the estimated model order classifies selected datasets into a single cluster ensuring the model could be generalized to the other datasets, and would be the most sensitive model order to structural changes.

$$\lambda = norm(\mathbf{R} - \mathbf{M}_R) \tag{6}$$

where $\mathbf{M}$ is a matrix of the mean of the vectors R_j ($j = 1, 2, ..., m$); R_j is a $n \times 1$ vector of the $\mathbf{R}$ parameters for j^{th} model order with n different datasets; λ is a $m \times 1$ vector.

2.3. Deterioration identification

In this study, a novel residual-based deterioration identification method is developed. The statistical hypotheses of chi-square variance test and two-sample t-test were conducted on residuals of time-series analyses. The deterioration features are defined as functions of the resulting T-values in the statistical hypotheses. The test statistics (T-values) are scalars of the probability of observing the test statistics as extreme as, or more extreme than, the observed values under the null hypotheses. Small values of T-values cast doubt on the validity of the null hypotheses. These hypotheses are conducted on residuals of time-series analyses resulting from the one-step-ahead error predictions, which are estimated in the baseline and assessment states of structures. If a structure does not change, the model should be able to appropriately predict the new signals in the assessment state assuming that the structural response is stationary. Hence, if a structure deteriorates, the new signal would be different from its prediction; in other words, the model fails to predict the signal well. The higher the structural changes are due to deterioration, the higher the residuals would be.

Chi-square variance test: This test used to test whether the variances of a population is equal to a hypothesis value. The test statistic is

$$T_1 = (n-1)\left(\frac{s_1}{s_2}\right)^2 \tag{7}$$

where s_1 and s_2 are the sample standard deviations of the baseline and test datasets, respectively, and n *is* the sample size.

Two-sample t-test: This test used to test whether two population means are equal. The test statistic is

$$T_2 = \frac{\mu_1 - \mu_2}{\sqrt{\frac{s_1^2}{n} + \frac{s_2^2}{n}}} \tag{8}$$

where μ_1 and μ_2 are the sample means of the baseline and test datasets, respectively.

To enhance the accuracy of the deterioration assessment method, the following integrated deterioration identification is defined by Equation 10. This equation ensures the sensitivity of the method to both changes in mean and variance of the response data due to deterioration.

$$T = \sqrt{T_1 \times T_2} \tag{9}$$

$$DI = \frac{|T_A - T_B|}{T_B} \tag{10}$$

where, T is the integrated tests statistics; A is the assessment condition and B is the baseline condition of structures.

Having notified of the deterioration identification requirement, a statistical evaluation is carried out to statistically determine the deterioration location. The following algorithm using Fisher criterion is used. The Fisher criterion f is given as:

$$f = \frac{(\mu_A - \mu_B)^2}{(\sigma_A)^2 + (\sigma_B)^2} \tag{11}$$

where μ and σ are the mean and the variance of the calculated *DI*, respectively; A is the assessment condition and B is the baseline condition of structures.

Fisher criterion is carried out to statistically determine the deterioration location and severity. It statistically measures the changes in the damage/deterioration features with respect to the reference condition of the structure. The sensor location associated with the largest Fisher criterion value could be identified as deterioration location (Mosavi et al.[20]). However, Fisher criterion is associated with some false positive and negative results. In order to enhance the fisher criterion method, *g* criterion is proposed as follows:

$$g_j = f_j - \frac{(\sum_{i=1}^{k} f_i) - f_j}{k-1} \geq 0 \tag{12}$$

where $j = 1, 2, ..., k$ and *k* is the number of sensor. This Equation cancels the false deterioration location from different sensors. The concept behind this equation is that small values of fisher criterion correspond to result from sensors far from the deterioration location. It should be noted that the *G* criterion is the *g* normalized. *G* =1 is corresponding to the location of deterioration.

$$G_j = \frac{g_j}{\max(g)} \tag{13}$$

2.3. Outlier removal via Hampel identifier

The previous study by the present authors[25] showed that the method can identify deterioration without false positive and negative results. However, those conclusions were based only on two simulation case studies. Data in real-world structures often contain outliers due to E&O variations and high measurement noise content. To remove these false positive and negative results, Hampel identifier is used to filter and clean the data. This filter-cleaner excludes outliers from the results without overly smoothing them and preserves all other information[47]. Removing outliers from results increases the accuracy of results. More information can be found in Hampel[48].

To summarise, first, the measured vibration response data is normalized. Then, AR time-series models fit the normalized data with proper model orders estimated using the proposed model identification technique. The proposed deterioration indicators are then calculated, and outliers are identified and removed from the results. Ultimately, deterioration is then identified by the proposed algorithms.

3. Case studies

3.1. Case study 1: Three (3) -storey RC frame

This is a finite element model (FEM) of a 3-storey reinforced concrete (RC) frame which was used in a previous paper of the present authors[25]. This 3-storey RC frame building (Figure 2) was designed and then modelled by computer program IDARC[49]. Dimensions of all columns and beams are $350\times350mm^2$ and $300\times300mm^2$, respectively. Table 1 shows the natural frequencies (f_e).

In this case study, the annual deterioration rate (ADR) of 2×10^{-3} is considered for the 50-year deterioration period. During this time, the cross-sectional areas of reinforcement bars of the left column at the first storey are gradually reduced[50] to simulate deterioration. Besides, at the age of 21 years old, this column experiences a slight damage. The slight damage is simulated as a sudden reduction in the cross-sectional area equal to 5 years of deterioration. The deterioration rate (DR) can be obtained by ADR times the duration of deterioration (DOD) process (in years). For more information see the previous paper of the current authors[25].

$$ADR = \left\{1 - \frac{Reduced\ cross\ sectional\ area}{Reference\ cross\ sectional\ area}\right\}_{year} \tag{14}$$

$$DR = ADR \times DOD \tag{15}$$

Table 1. Dimensions of columns and beams

Mode	f_e (Hz)
1st	2.16
2nd	7.68
3rd	15.75

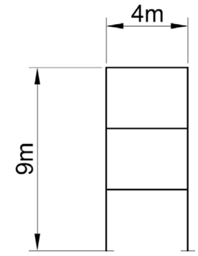

Figure 2. 3-storey RC frame

The effect of the deterioration on the dynamic characteristics and frequency content are illustrated in Figure 3. This figure shows periodogram power spectral density (PSD) estimate of the response data for the frame with the healthy state and 50 years of deterioration. PSD calculates the significance of different frequencies in time-series data. Athough the PSD of a deterirorated structure may appear more noisy than that of the healthy structure, the peak frequencies can be seen very close between these two cases. It can be concluded that, frequency domain methods are not effective to detect small structural changes such as the deterioration investigated in the current study.Therefore, only the AR time-series approach will be applied in the next case studies.

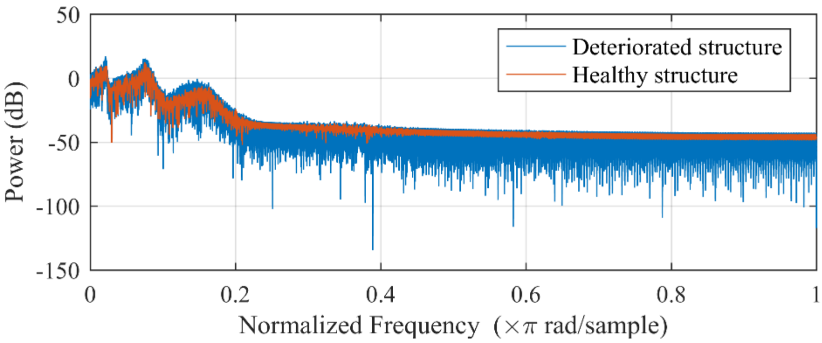

Figure 3. Periodogram power spectral density (PSD) estimate

The response data of a real structure[51] under ambient vibrations with a sampling frequency of 2000Hz and sample size of 120000 data points are used as input ambient excitations for the simulated RC frame. Then, the response acceleration data of the simulated structure with the mentioned deterioration cases are utilized as input data for the proposed method. The response acceleration data are decimated using a factor of ten in order to mitigate the high-frequency content[42,52]. It reduces the original sample frequency of 2000Hz down to 200Hz. Then, a 10% white Gaussian noise is added to the data. The contaminated data with noise simulates the recorded sensor data in real-world conditions. Then the normalization procedure is conducted. The normalized data is then modelled as AR time-series models. For a proper AR estimation and enhancing the sensitivity of the time-series based deterioration evaluation, OMO technique is used. Finally, the deterioration identification is calculated using equation 14. Possible outliers are then removed using Hampel filter-cleaner.

The proposed OMO technique is performed on 1440 datasets in the baseline state in order to estimate optimal model orders for each sensor data. The optimal model orders are chosen in a range of 1 to 40. Figure 4a illustrates γ criterion of AR models for all the considered baseline datasets (1440 datasets). This criterion suggests that the minimum model order of 10 is required to fit well the time history, since γ parameter is minimized and almost constant with model orders higher than ten. This model order satisfies the minimum complexity of time-series models[52]. The optimal model order corresponds to the minimum of λ parameter for model orders higher than the minimum model order obtained from γ parameter (Figure 4b). This figure shows that the optimum model order for the used datasets is 14 (the model order corresponding to the minimum γ parameter for model orders higher than 10). It is important to note that the optimal model order should be separately estimated for each sensor.

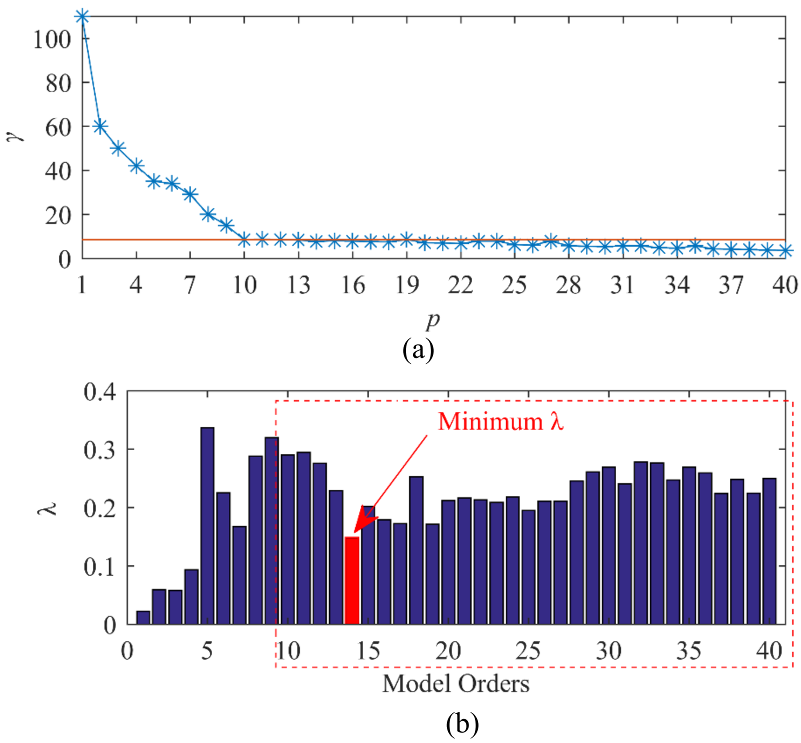

Figure 4. OMO technique: (a) γ parameter, (b) λ parameter

Estimating the proper model order is the key to precisely identify deterioration. Figure 5 shows the effect of different model orders on *DI*. As shown above, the optimal model order for the chosen datasets is 14. A higher model order, for instance order of 30, increases the residuals and results in false positive and negative values. On the other hand, a lower model order, for example model order of 7, fails to identify deterioration.

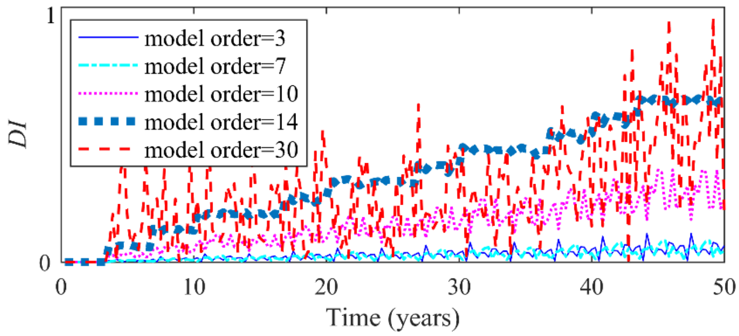

Figure 5. Effect of different model orders on *DI*

Results of the deterioration assessment of the simulated deterioration are presented in Figure 6. It shows that the proposed method is able to detect deterioration and sudden damage. *DI* values are zero when the frame is just built (time=0). By the time at which the structure experienced deterioration, the *DI* increases in time. At the age of 21 years, the method clearly detects the slight, but sudden damage.

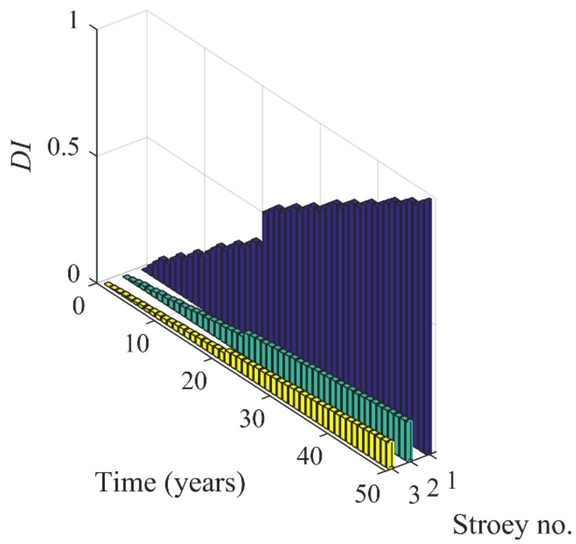

Figure 6. Deterioration identification

To locate deterioration, a novel fisher criterion-based method is proposed in the current study. This method uses the *DI* values calculated in the deterioration detection method. So as to cancel any false positive/negative results in deterioration localization due to using the fisher criterion, Equations 14 is proposed. This equation cancels all the non-zero but low values of fisher criterion. The concept behind this method is that fisher criterion gives higher values when deterioration location is closer to the sensor. Figure 7 clearly illustrates that the proposed method clearly locates deterioration in the 1st storey.

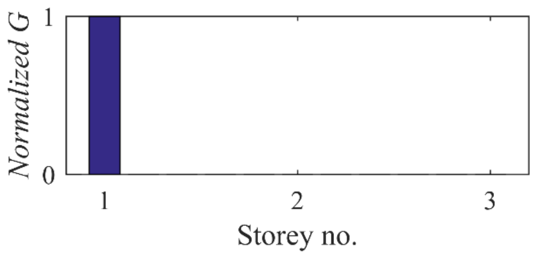

Figure 7. Deterioration location

3.2. Case study 2: the 20-storey RC frame

The 20-storey RC frame is a FEM model which was used in the previous paper of the present authors[25]. Table 2 presents the dimensions of this 4 span frame (Figure 8) which is modelled by computer program IDARC[49]. Table 3 shows the first seven natural frequencies (f_e).The same data with the sampling frequency of 2000Hz and the sample size of 120000 data points (sample length was 120000/60=60 seconds) are used to excite the model and record the structural responses.

Table 2. Dimensions of columns and beams

	BEAM		COLUMN	
STOREY	Dimensions (mm)	Steel area (mm^2)	Dimensions (mm)	Steel area (mm^2)
16-20	400*400	900	400*400	4560
11-15	450*450	900	500*500	7385
6-10	500*500	900	600*600	9646
1-5	550*550	1000	700*700	9646

Table 3. The first seven natural frequencies in Hz

MODE	1ST	2ND	3RD	4TH	5TH	6TH	7TH
(HZ)	0.54	1.5	2.5	3.8	5	6.45	8.04

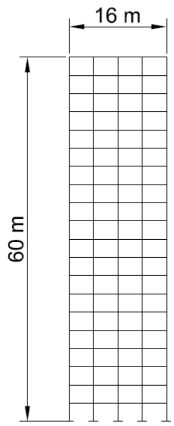

Figure 8. 20-storey RC frame

Similarly, deterioration is simulated with ADR for 50 years of deterioration. During this period, the cross-sectional areas of reinforcement bars of the left columns are gradually reduced[50] according to the deterioration scenarios (Table 4). In scenario #1, the left column at level 10 experiences deterioration but not damage for 50 years. In scenario #2, the left columns at levels 5 and 15 experience deterioration for 50 years and preventive damage maintenances at the age of 28 years. In scenario #3, the left columns at levels 3, 8, 14 and 20 experience deterioration for 50 years and slight preventive damage maintenances at the age of 32.

Table 4. Deterioration scenarios

SCENARIOS	STORIES	EXPLANATIONS
1	10	50-year deterioration
2	5 & 15	50-year deterioration & maintenances at the age of 28

3	3,8,14 & 20	50-year deterioration & maintenances at the age of 32

Similar to the previous case study, the response data of the real structure[51] under ambient vibration with the same sampling frequency and sample size are used as input ambient excitations. Then, the response acceleration data of the simulated deteriorated structure are utilized as input data for the proposed method. Furthermore, white Gaussian noise with the signal-to-noise ratio per sample of 10 (10% noise) is added. Then, the data normalization procedure is conducted. The optimal model orders are estimated for each sensor channel using the proposed OMO technique. The acceleration response data are then modelled as AR time-series. Finally, possible outliers are removed from the calculated *DI* using Hampel filter-cleaner.

The results of the deterioration assessment under the three different scenarios are presented in Figures 9 to 11. These figures show that the proposed method clearly detects the simulated deterioration and preventive damage maintenances in all scenarios. *DI* shows zero value when the frame is just built (time=0). By deterioration of the structure in the 50-year time period, the *DI* clearly shows increasing deterioration in the structure. In scenario #1, the structure deteriorates for 50 years at the 10^{th} floor. The results in Figure 9 clearly show that the proposed method clearly detects deterioration of the frame for 50 years at the 10^{th} floor. The *DI* increases in time due to accumulation of deterioration in time. In scenario #2, the structure starts deterioration at the 5^{th} and 15^{th} floors. Then, preventive maintenance actions are performed in both floors at the age of 28, in which the method clearly detects and depicts both deterioration and the maintenance actions (see Figure 10). The latter can be seen as a sudden decrease in the *DI* values. In scenario #3, the method detects a progressive and steady deterioration trend at first. Then, at the age of 32 the slight preventive maintenance actions are detected as shown in Figure 11. Besides, it is evident that deterioration in each storey affects the DI results of other stories. However, the *DI* values are greater when the sensor location is closer to deterioration location.

The results of *G* criterion (Equation 15) for locating deterioration are depicted in Figure 12. It is verified that the proposed method can clearly locate deterioration. Figure 12a clearly shows that in scenario #1, the 10^{th} storey has deteriorated. In scenario #2, the 5^{th} and 15^{th} floors deteriorated. Figure 12b shows the same results. In scenario #3, all the 3^{rd}, 8^{th}, 14^{th} and 20^{th} floors are deteriorated, and the deterioration localization method clearly detects deterioration in these floors in Figure 12c. As a result, it can be concluded that the proposed method can clearly detect and locate deterioration.

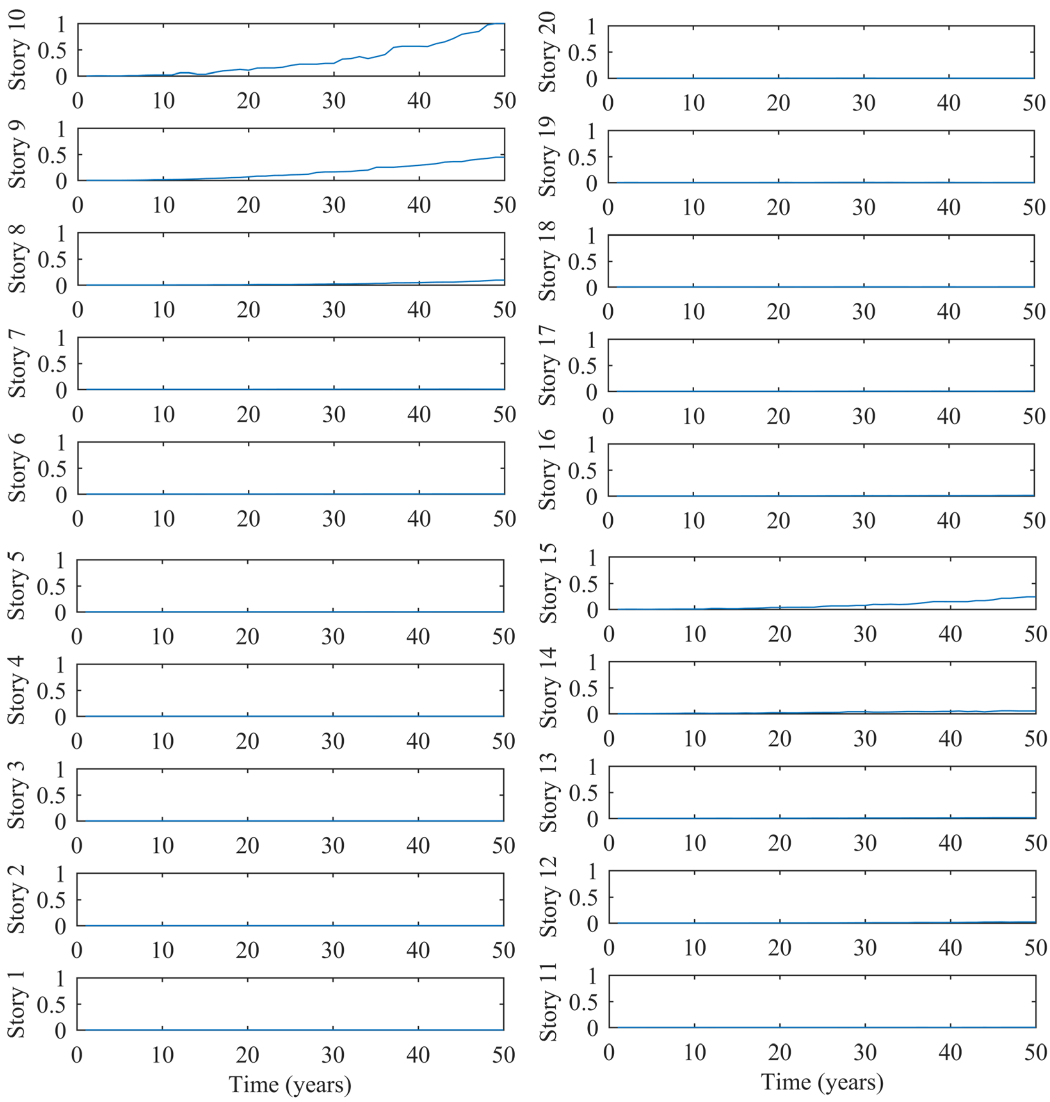

Figure 9. Deterioration identification, scenario #1

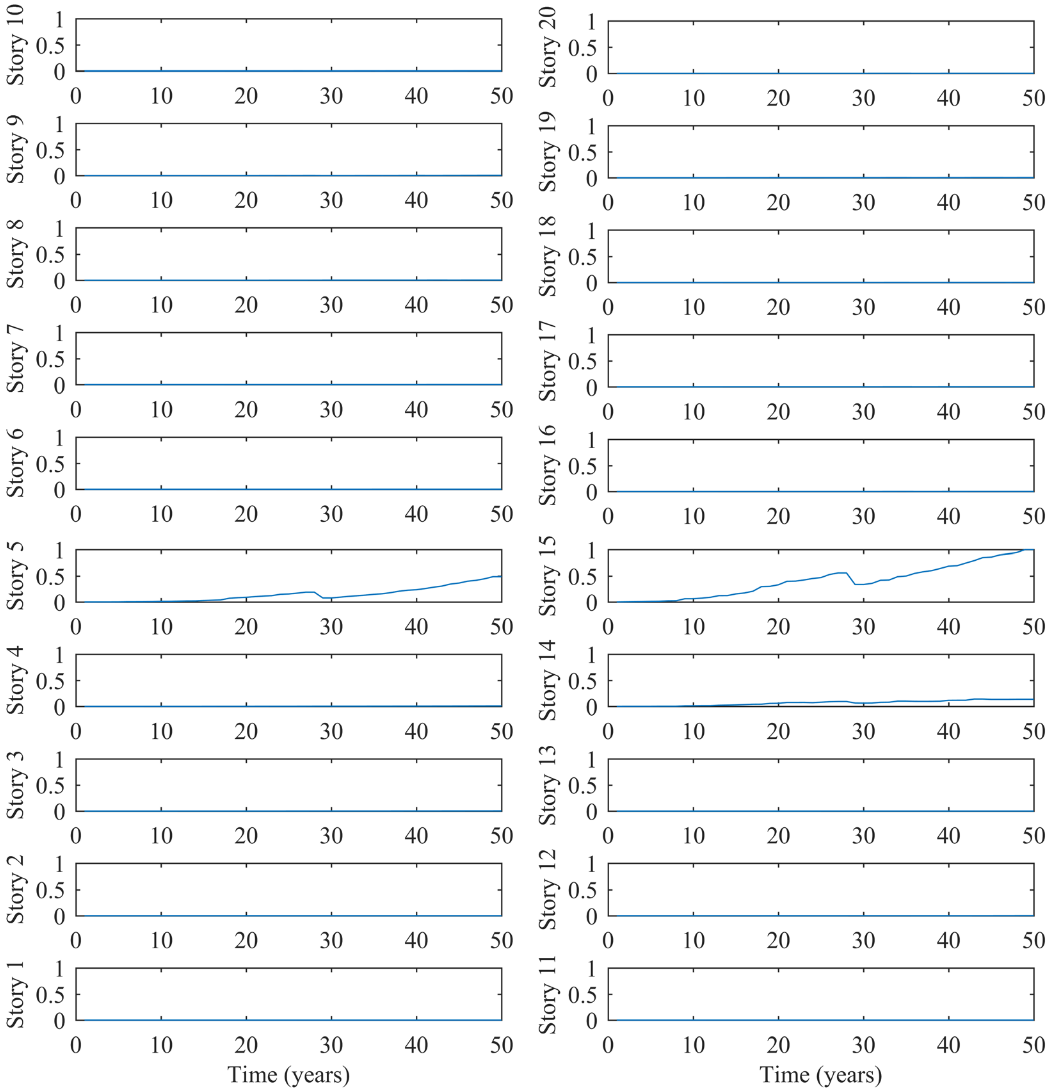

Figure 10. Deterioration identification scenario #2

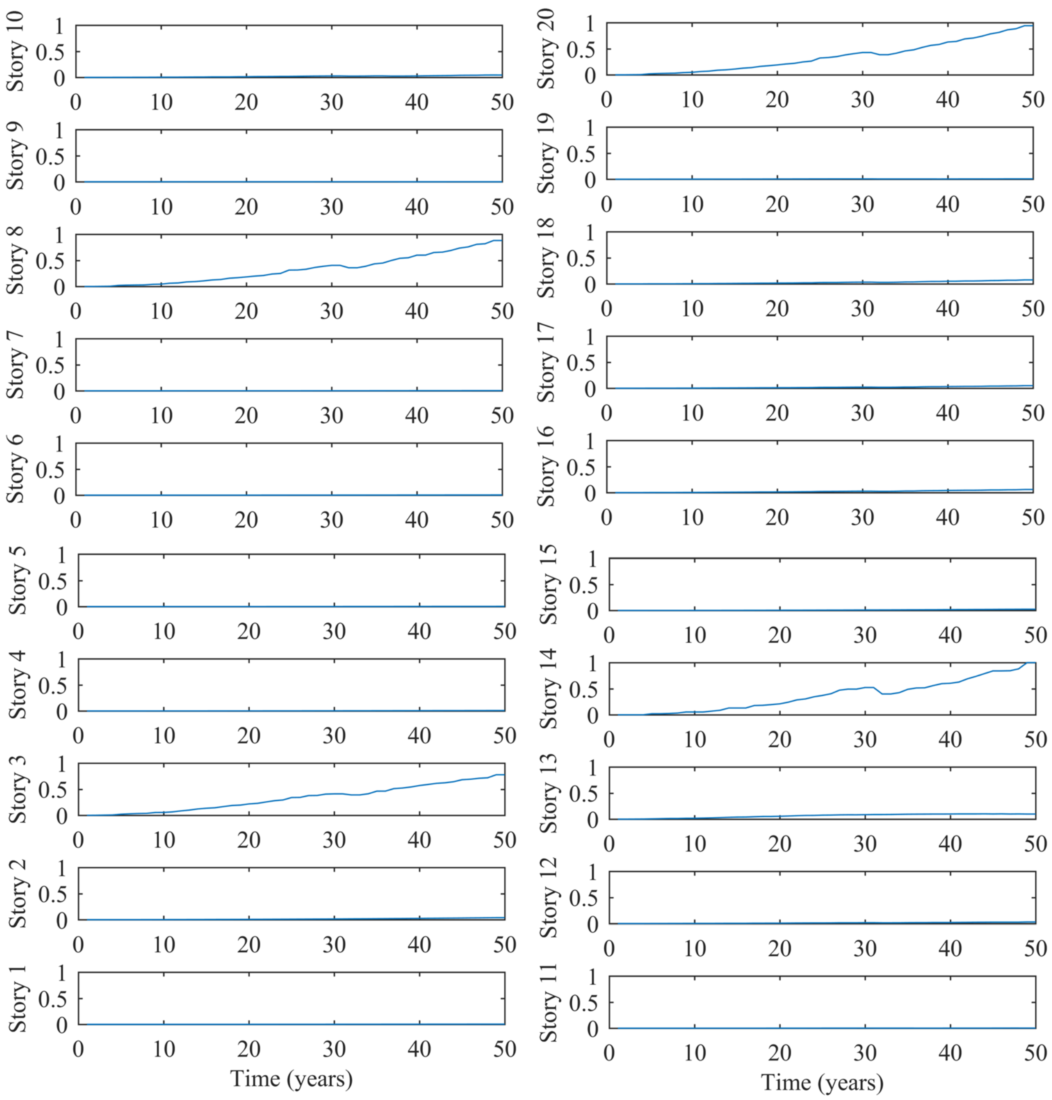

Figure 11. Deterioration identification scenario #3

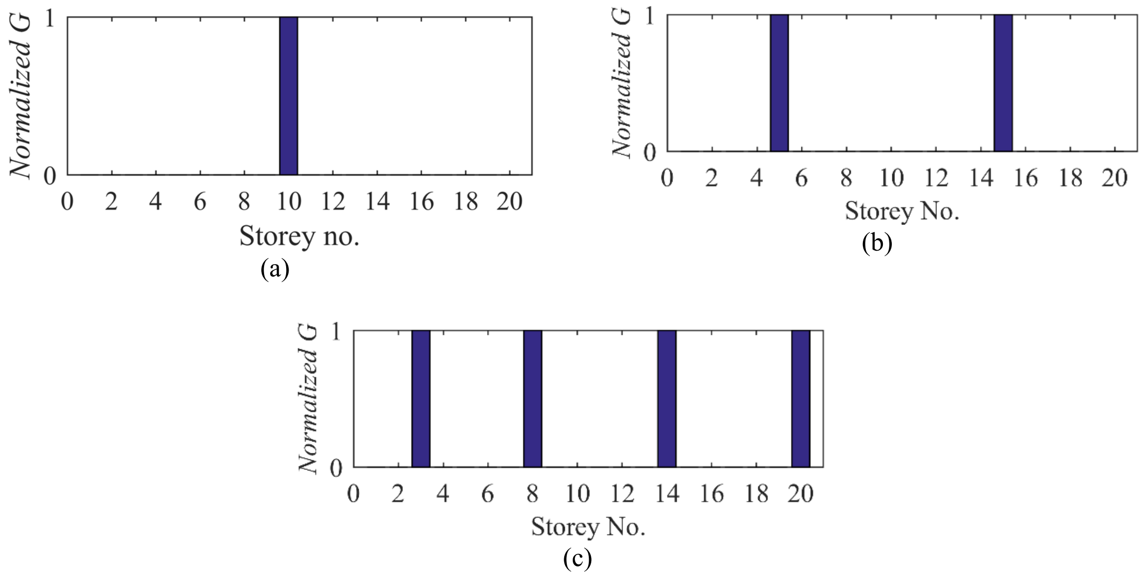

Figure 12. Deterioration location (a) scenario #1; (b) scenario #2; (c) scenario #3

3.3. Case study 3: box-girder bridge structure

The proposed method in the current study is experimentally validated using sensor data from a test on a large-scale BGB structure. The BGB structure was constructed to study the pre-stress force identifications in pre-stressed concrete BGBs[53], then load-carrying capacity assessment[54] and damage detection elsewhere before being used for deterioration detection validation in the present study.

This simply supported BGB model is 6m long and 5.8m long between the supports. The pre-stressing tendons of the model are removed before the tests. Figures 13a shows the actual BGB test setup while Figures 13b and 13c show the detailed dimensions of the BGB structure. In Figure 13c, A to I indicate positions where the sensors are attached.

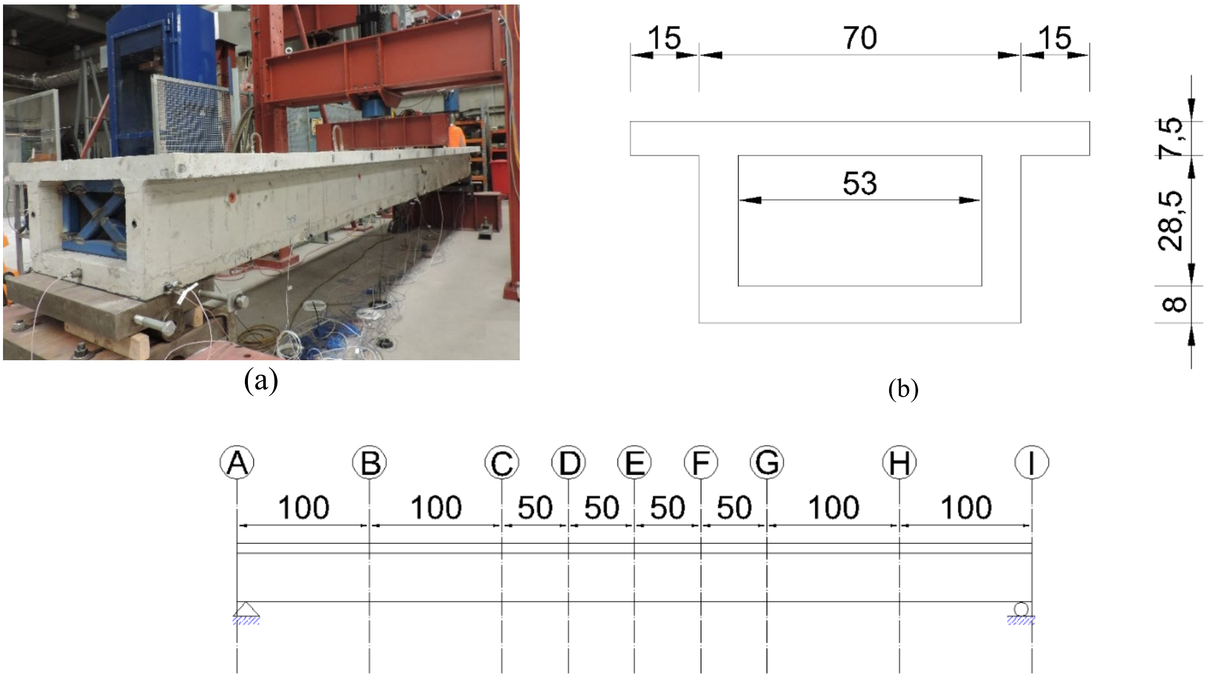

(a)

(b)

(c) A to I indicate positions of accelerometers

Figure 13. The box-girder model (a) test setup, (b) cross-section, (c) detailed dimensions (all dimensions are in cm).

The box-girder model is excited by hitting randomly along the length of the model by an impact hammer to simulate ambient vibration. 18 accelerometers are attached to the structure to measure its response according to the sensor layout shown in Figure 14. This figure shows the detailed model of the BGB structure modelled by ARTeMIS software[55]. The numbers beside each sensor indicate the sensor number. For instance, sensor 6 is located at section C on the top flange. A centralised data acquisition system and an in-house software program based on National Instruments hardware and software (LabVIEW) are used to collect and record the data[56]. The analogue sensor data are recorded continuously for approximate 2 minutes and discretised to computer hard disk at a sampling frequency of 2048 Hz.

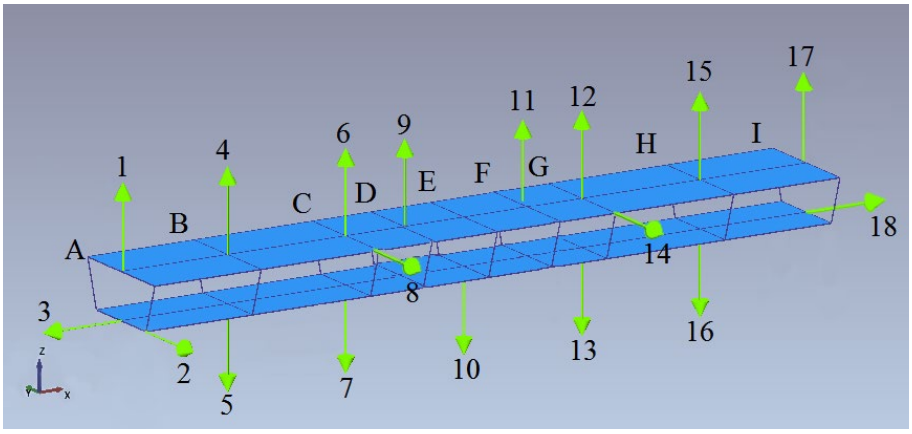

Figure 14. The box-girder sensor arrangement

The experiment is conducted in three different structural state conditions. In the first state (test 01), the BGB model is under baseline conditions. In order to simulate the second structural state (test 02), static and cyclic loads are applied at the mid-span of the two girders using Moog system as shown in Figure 15. Some very small cracks, which could be hardly seen without using a magnifying glass, occurred at the bottom flange and the lower part of the webs (Figure 16). The third structural state (test 03) is created by applying further static loads at the same position. The previous cracks are lengthened to the near top part of the webs and some new cracks are developed (Figure 17). It should be noted that these cracks are very small and they could be hardly seen or noticed. Figure 18 shows a developed crack in test 02. As shown, this crack can be hardly seen (Figure 18a). In order to enhance the visibility of this crack, image processing is conducted (Figure 18b). Figures 19a and 19b show a lengthened crack in test 03. As shown in Figure 19b, after image processing, a new crack is detected. Since these cracks could hardly be visible, they were highlighted by a yellow marker on the BGB structure.

The response acceleration data from each sensor are measured and recorded during the conducted tests and normalized afterwards. The proposed OMO technique is then applied on the normalized data to estimate optimal model order for each sensor. The response data are modelled as AR time-series, and deterioration indicator is defined using the *T*-values of the statistical hypothesis of chi-square variance test. The deterioration assessment results of some sensors are shown in Figure 20. It should be noted that datasets 1 to 70, 71 to 197 and 198 to 316 correspond to test 01, test 02 and test 03, respectively. The results clearly show that the proposed method successfully detected deterioration and the sudden damage in this real-world structures. *DI* values are zero in average at the baseline condition (test 01). *DI* increases in test

02 and test 03 due to changes in the state conditions. Moreover, the slight increase in the trend during test 02 suggests that the BGB structure is deteriorating during this time due to external forces.

Figure 15. The Moog system

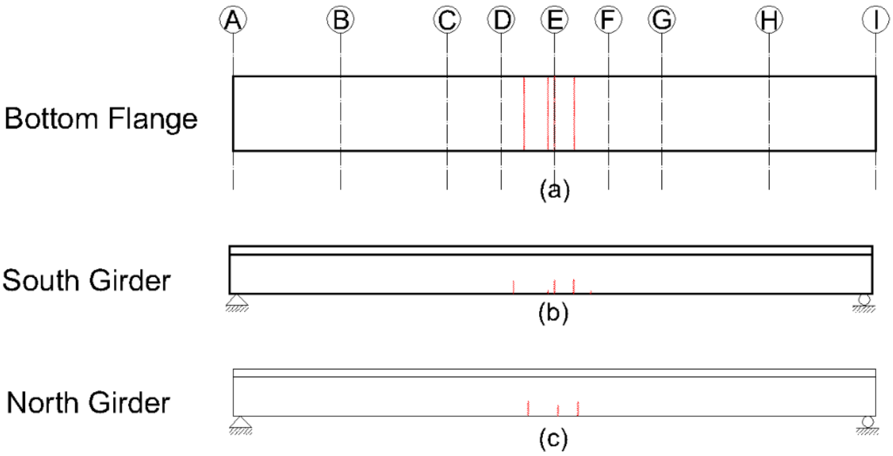

Figure 16. Crack distribution in test 02 at (a) bottom flange, (b) South girder, (c) North girder

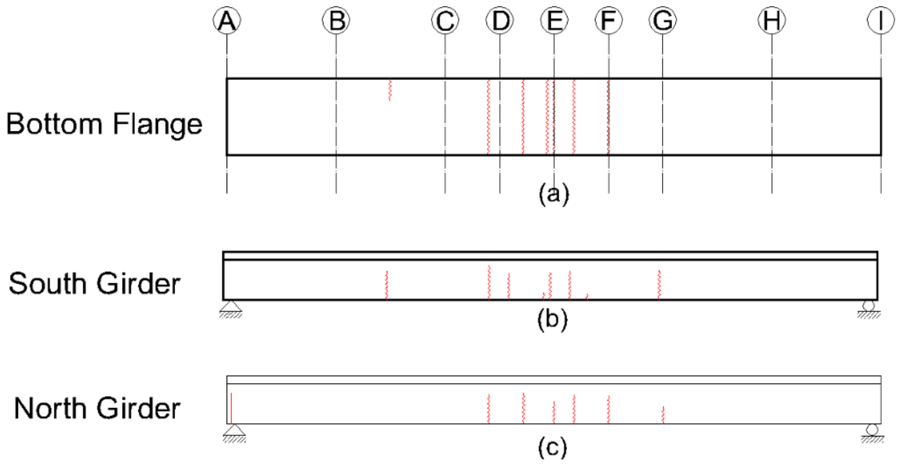

Figure 17. Crack distribution in test 03 at (a) bottom flange, (b) South girder, (c) North girder

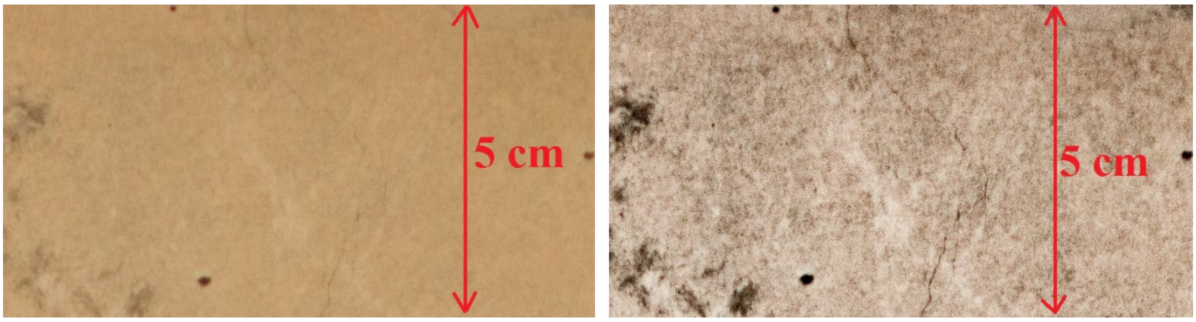

(a) (b)

Figure 18. A developed crack in test 02: (a) the original image (b) the processed image

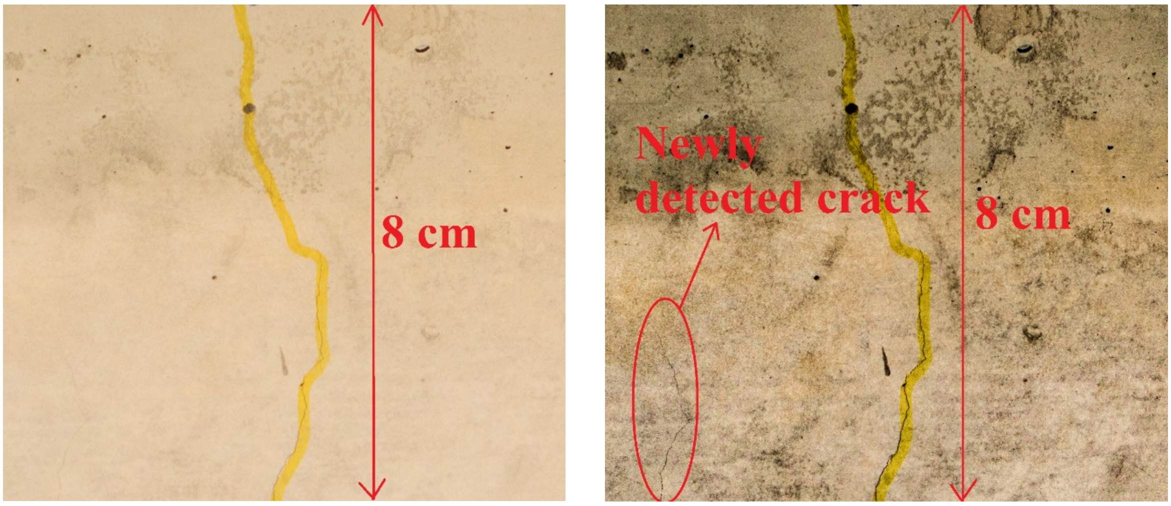

(a) (b)

Figure 19. A developed crack in test 03: (a) the original image (b) the processed image

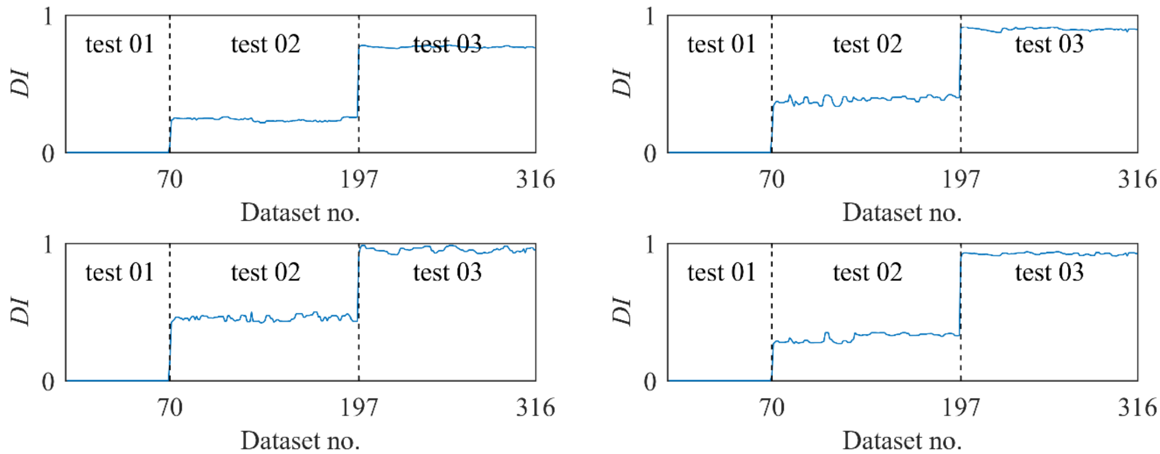

Figure 20. Deterioration identification in the box-girder model

Deterioration locations were estimated using the proposed method in this study. Results of *G* criterion for locating deterioration in test 02 are shown in Figure 21. It is verified that the proposed method can clearly locate deterioration. This figure clearly shows that the proposed method is able to locate very small cracks. For instance, in test 02, only a few cracks were developed in the middle span (points D, E and F), and in state #3, the cracks lengthened and more cracks developed in other locations (points A, C, D, E, F and G).

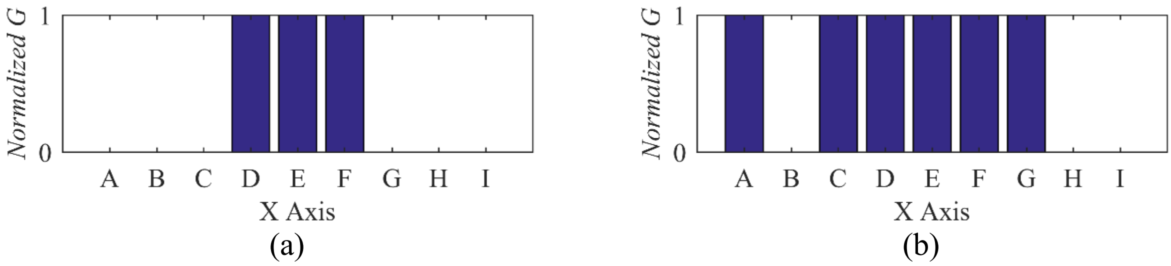

Figure 21. Deterioration location on the box-girder in (a) test 02 (b) test 03

4. Further Discussions

4.1. Noise content

In order to illustrate the efficiency of the proposed method in the current study, similar to the case study 1, the response acceleration data of the simulated deteriorated frame is utilized as input data for the proposed method, and different white Gaussian noise of 2%, 5%, 10%, 15% and 20% are added to the data. Equation 16 is used to simulate a linear deterioration in time with a slight but sudden damage in year 16. The results of the deterioration identification are shown in Figure 22 which demonstrates that the proposed method is able to detect deterioration and sudden damage in the presence of high noise content. The noise in the data had a negligible impact on the results and validated the efficiency of the proposed methodology developed in the current study.

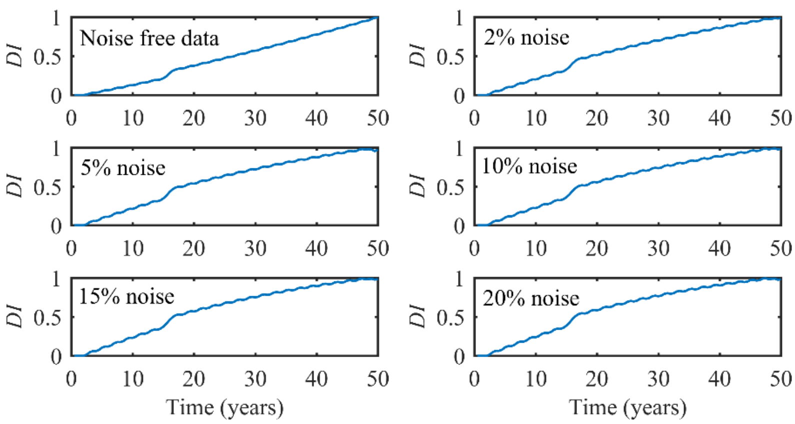

Figure 22. Deterioration identification under different noise content

4.2. Outlier removal

In order to investigate the effects of removing the outliers via Hampel identifier, the deterioration assessment results with and without outliers are represented in Figure 23. In this figure, data from case study 3 (BGB structure) are used. This figure illustrates that Hampel identifier successfully removed all the false positive and negative results. The results indicate that Hampel filter-cleaner only removes the outliers. In other words, if the structural characteristics change due to deterioration or damage, the filter does not remove the *DI* changes.

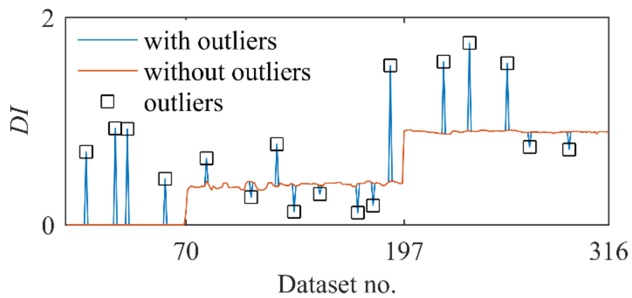

Figure 23. Outlier removal effects on deterioration identification results

4.3. Sample length

In a recently published paper of the current authors[25], different sample lengths were tested in two numerical case studies. They concluded that the sample length has a negligible effect on their deterioration assessment method. In order to test time series based deterioration identification methods in real structures, this study used different sample lengths in the experimental case study in order to further investigate their impact on the deterioration evaluation (see Figure 24). Results show that sample length has a negligible impact on the proposed deterioration identification method.

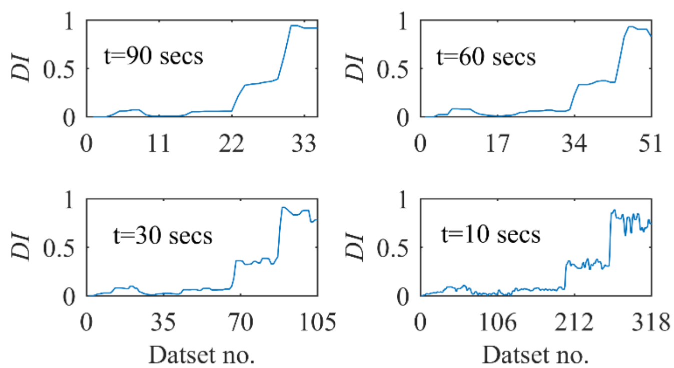

Figure 24. Deterioration identification using different sample lengths

5. Conclusion

The main contribution of this study is the development and application of an integrated deterioration assessment method, which for the first time enables structural deterioration to be globally detected and located using a vibration-based method. This method is based on time-series analysis, statistical hypotheses, Hampel identifier and Fisher criterion. A normalization procedure and a model identification technique are also developed to enhance time series analysis to achieve deterioration identification. Acceleration data from two simulation case studies of 3-storey and 20-storey RC frames and one experimental dataset from a BGB structure are adopted to assess the efficiency and robustness of the new deterioration identification method proposed in this study. The results show that: 1) the developed method is capable of detecting and locating deterioration. 2) Time-series model orders play a crucial role in detecting small changes in dynamic characteristics of structures. 3) The method is able to detect sudden structural changes due to damage, preventive maintenance actions, cumulative deterioration or other external excitation sources, such as blast and earthquake. 4) The proposed method is able to identify deterioration in the presence of high level of noise content. 5) Hampel identifier successfully removes all the false positive and negative results. 6) Sample length had a negligible impact on the proposed deterioration identification method. 7) The method does not require data from deteriorated states to be available beforehand. 8) The method can be used to assess deterioration in real-time.

Although the method showed great success in deterioration assessment, some challenges remain to be addressed in the future studies, including developing the method to be able to estimate the severity of deterioration and to provide early warning before damage due to accumulated deterioration. Any information on the possible time and location of structural damage due to accumulated deterioration can improve safety of structures, enhance their performance and save time and money.

Acknowledgements

The first author gratefully appreciates the financial support for his research from the Queensland University of Technology (QUT) and School of Civil Engineering and Built Environment. Experimental data used in the third case study is from the load-carrying capacity test done by Shojaeddin Jamali as part of his PhD. The research herein is part of Discovery Project DP160101764 funded by the Australian Government through the Australian Research Council (ARC).

REFERENCES

1. D. Saydam and D. M. Frangopol, Time-dependent performance indicators of damaged bridge superstructures, *Eng. Struct.* **33**(9) (2011) 2458-2471.
2. D. V. Val and M. G. Stewart, Decision analysis for deteriorating structures, *Reliab. Eng. Syst. Safe.* **87**(3) (2005) 377-385.
3. Y. Liu, Doctoral dissertation, Virginia Tech, 1996.
4. D. M. Frangopol and M. Soliman, Life-cycle of structural systems: recent achievements and future directions, *Struct. Infrastruct. Eng.*) (2015) 1-20.
5. Sanchez-Silva, M., Klutke, G. A., & Rosowsky, D. V., Life-cycle performance of structures subject to multiple deterioration mechanisms, *Struct. Saf.* ***33***(3) (2011) 206-217.
6. Berto, L., Vitaliani, R., Saetta, A., & Simioni, P., Seismic assessment of existing RC structures affected by degradation phenomena, *Struct. Saf.* **31**(4) (2009) 284-297.
7. Gulikers, J., Theoretical considerations on the supposed linear relationship between concrete resistivity and corrosion rate of steel reinforcement, *Mater. Corros.* ***56***(6) (2005) 393-403.
8. Morinaga, S., Prediction of service lives of reinforced concrete buildings based on rate of corrosion of reinforcing steel, *Special report of Institute of Technology, Shimizu Corporation* (23) (1988).
9. Wang, X. H., & Liu, X. L., Modelling effects of corrosion on cover cracking and bond in reinforced concrete. *Magazine of Concrete Research* **56**(4) (2004) 191-199.
10. Okasha, N. M., & Frangopol, D. M., Time-variant redundancy of structural systems. *Struct. Infrastruct. E.* **6**(1-2) (2010) 279-301.
11. Barone, G., Frangopol, D. M., & Soliman, M., Optimization of Life-Cycle Maintenance of Deteriorating Bridges with Respect to Expected Annual System Failure Rate and Expected Cumulative Cost, *J. Struct. Eng.* **140**(2) (2014) 04013043.
12. Zhou, Z., *Vibration-based damage detection of simple bridge superstructures.* (PhD), University of Saskatchewan (2006).
13. S. W. Doebling, C. R. Farrar and M. B. Prime, A summary review of vibration-based damage identification methods, *Shock Vib. Dig.* **30**(2) (1998) 91-105.
14. E. P. Carden and P. Fanning, Vibration based condition monitoring: a review, *Struct. Health Monit.* **3**(4) (2004) 355-377.
15. T. H. T. Chan and D. P. Thambiratnam, Structural health monitoring in Australia, Nova Science Publishers, (2011).
16. C. R. Farrar and D. A. Jauregui, Comparative study of damage identification algorithms applied to a bridge: II. Numerical study, *Smart Mater. Struct.* **7**(5) (1998) 720-731.
17. C. R. Farrar and D. A. Jauregui, Comparative study of damage identification algorithms applied to a bridge: I. Experiment, *Smart Mater. Struct.* **7**(5) (1998) 704-719.
18. H. W. Shih, D. P. Thambiratnam and T. H. T. Chan, Vibration based structural damage detection in flexural members using multi-criteria approach, *J. Sound Vib.* **323**(3-5) (2009) 645-661.
19. A. Alvandi and C. Cremona, Assessment of vibration-based damage identification techniques, *J. Sound Vib.* **292**(1) (2006) 179-202.
20. A. A. Mosavi, D. Dickey, R. Seracino and S. Rizkalla, Identifying damage locations under ambient vibrations utilizing vector autoregressive models and Mahalanobis distances, *Mech. Syst. Sig. Process.* **26** (2012) 254-267.
21. U. Kadakal and O. Yuzugullu, A comparative study on the identification methods for the autoregressive modelling from the ambient vibration records, *Soil Dyn. Earthquake Eng.* **15**(1) (1996) 45-49.
22. G. C. Pardoen, Ambient Vibration Test-Results of the Imperial-County-Services-Building, *B. Seismol. Soc. Am.* **73**(6) (1983) 1895-1902.

23. B. Monavari, T. H. T. Chan, A. Nguyen and D. Thambiratnam, Time-Series Coefficient-Based Deterioration Detection Algorithm, *The 8th International Conference on Structural Health Monitoring of Intelligent Infrastructure (SHMII-08)*, *Curran Associates, Inc.*, Brisbane, Australia (2017) 1232-1240.
24. B. Monavari, T. H. T. Chan, A. Nguyen and D. Thambiratnam, Deterioration Sensitive Feature using Enhanced AR Model Residuals, *Fourth Conference on Smart Monitoring, Assessment and Rehabilitation of Civil Structures*, Zurich, Sweetzerland (2017).
25. B. Monavari, T. H. T. Chan, A. Nguyen and D. Thambiratnam, Structural Deterioration Detection Using Enhanced Autoregressive Residuals, *Int. J. Struct. Stab. Dy.* **18**(12) (2018)
26. M. L. Fugate, H. Sohn and C. R. Farrar, Vibration-based damage detection using statistical process control, *Mech. Syst. Sig. Process.* **15**(4) (2001) 707-721.
27. C. S. Sakaris, J. S. Sakellariou and S. D. Fassois, Vibration-based damage precise localization in three-dimensional structures: Single versus multiple response measurements, *Struct. Health Monit.* **14**(3) (2015) 300-314.
28. H. Sohn, D. W. Allen, K. Worden and C. R. Farrar, Statistical damage classification using sequential probability ratio tests, *Struct. Health Monit.* **2**(1) (2003) 57-74.
29. O. R. de Lautour and P. Omenzetter, Nearest neighbor and learning vector quantization classification for damage detection using time series analysis, *Struct. Control. Hlth.* **17**(6) (2009) 614-631.
30. O. R. de Lautour and P. Omenzetter, Damage classification and estimation in experimental structures using time series analysis and pattern recognition, *Mech. Syst. Sig. Process.* **24**(5) (2010) 1556-1569.
31. Carden, E. P., & Brownjohn, J. M. W., ARMA modelled time-series classification for structural health monitoring of civil infrastructure, *Mech. Syst. Signal. Pr.* **22**(2) (2008) 295-314.
32. Pandit, S. M., & Wu, S. M., *Time series and system analysis with applications*: Wiley New York (1983).
33. Garcia, G. V., & Osegueda, R. A., *Damage detection using ARMA model coefficients.* Paper presented at the 1999 Symposium on Smart Structures and Materials (1999).
34. Mei, L., Li, H., Zhou, Y., Wang, W., & Xing, F., Substructural damage detection in shear structures via ARMAX model and optimal subpattern assignment distance, *Eng. Struct.* **191** (2019) 625-639.
35. Do, N. T., & Gül, M., A time series based damage detection method for obtaining separate mass and stiffness damage features of shear-type structures, *Eng. Struct.* 109914.
36. Ay, A. M., & Wang, Y., Structural damage identification based on self-fitting ARMAX model and multi-sensor data fusion, *Struct. Health Monit.* **13**(4) (2014) 445-460.
37. E. Zugasti, J. Anduaga and M. A. Arregui, NullSpace and AutoRegressive damage detection: a comparative study, *Smart Mater. Struct.* **21**(8) (2012) 085010.
38. P. Omenzetter and J. M. W. Brownjohn, Application of time series analysis for bridge monitoring, *Smart Mater. Struct.* **15**(1) (2006) 129-138.
39. Q. W. Zhang, Statistical damage identification for bridges using ambient vibration data, *Comput. Struct.* **85**(7-8) (2007) 476-485.
40. Z. Wang, F. Liu, Lian Q. Yu and Shuang H. Chen, Structural Damage Detection Using Sensitivity-Enhanced Autoregressive Coefficients, *Int. J. Struct. Stab. Dy.* **16**(03) (2016) 1550001.
41. H. Zheng and A. Mita, Localized damage detection of structures subject to multiple ambient excitations using two distance measures for autoregressive models, *Struct. Health Monit.* **8**(3) (2009) 207-222.
42. S. W. Smith, The scientist and engineer's guide to digital signal processing, California Technical Publishing San Diego, CA, USA (1997).
43. A. Cichocki and S. Amari, Adaptive Blind Signal and Image Processing, West Sussex: John Wiley & Sons, (2002).

44. E. Figueiredo, J. Figueiras, G. Park, C. R. Farrar and K. Worden, Influence of the Autoregressive Model Order on Damage Detection, *Comput.-Aided Civ. Infrastruct. Eng.* **26**(3) (2011) 225-238.

45. G. E. P. Box, G. M. Jenkins and G. C. Rensel, Time Series Analysis: Forecasting and Control, John Wiley & Sons, (2008).

46. A. Entezami and H. Shariatmadar, An unsupervised learning approach by novel damage indices in structural health monitoring for damage localization and quantification, *Struct. Health Monit.* **17**(2) (2017) 325-345.

47. H. Liu, S. Shah and W. Jiang, On-line outlier detection and data cleaning, *Computers and Chemical Engineering* **28**(9) (2004) 1635-1647.

48. F. R. Hampel, The influence curve and its role in robust estimation, *Journal of the American Statistical Association* **69** (1974) 382–393.

49. A. M. Reinhorn, H. Roh, M. V. Sivaselvan, S. K. Kunnath, R. E. Valles, A. Madan, C. Li, R. F. Lobo and P. Y. J., IDARC2D, version 7.0: A Program for the Inelastic Damage Analysis of Structures, University of Buffalo, NY, USA (2009).

50. N. M. Okasha and D. M. Frangopol, Time-variant redundancy of structural systems, *Struct. Infrastruct. Eng.* **6**(1-2) (2010) 279-301.

51. T. Nguyen, T. H. T. Chan, D. P. Thambiratnam and L. King, Development of a cost-effective and flexible vibration DAQ system for long-term continuous structural health monitoring, *Mech. Syst. Sig. Process.* **64** (2015) 313-324.

52. E. Figueiredo, G. Park, J. Figueiras, C. Farrar and K. Worden, Structural Health Monitoring Algorithm Comparisons Using Standard Data Sets, Los Alamos National Laboratory (LANL), Los Alamos, NM, United States (2009).

53. T. S. Pathirage, Queensland University of Technology, 2017.

54. Jamali, S., Chan, T. H., Nguyen, A., & Thambiratnam, D. P., Reliability-based load-carrying capacity assessment of bridges using structural health monitoring and nonlinear analysis, *Struct. Health Monit.* **18**(1) (2019) 20-34.

55. ARTeMIS Modal 4.0 (Computer software), Issued by Structural Vibration Solutions A/S, NOVI Science Park, Niels Jernes Vej 10, DK 9220 Aalborg East, Denmark (2015).

56. A. Nguyen, T. H. T. Chan and D. Thambiratnam, Output-only modal testing and monitoring of civil engineering structures: Instrumentation and test management, *The 8th International Conference on Structural Health Monitoring of Intelligent Infrastructure (SHMII-08)*, *Curran Associates, Inc.*, Brisbane, Australia (2017) 1-12.